Ground-state structure and stability of dipolar condensates in anisotropic traps

O. Dutta* and P. Meystre
Department of Physics and College of Optical Sciences, University of Arizona, Tucson, Arizona 85721, USA
(Received 28 February 2007; published 9 May 2007)

We study the Hartree ground state of a dipolar condensate of atoms or molecules in a three-dimensional anisotropic geometry and at $T=0$. We determine the stability of the condensate as a function of the aspect ratios of the trap frequencies and of the dipolar strength. We find numerically a rich phase space structure characterized by various structures of the ground-state density profile.

DOI: 10.1103/PhysRevA.75.053604 PACS number(s): 03.75.Hh

I. INTRODUCTION

The realization of Bose-Einstein condensation (BEC) in low-density atomic vapors [1,2] has led to an explosion of experimental and theoretical research on the physics of quantum-degenerate atomic and molecular systems. While much of the work so far has concentrated on systems characterized by *s*-wave two-body interactions, the recent demonstration of a condensate of chromium atoms [3] opens up the study of gases that interact via long-range, anisotropic magnetic dipole interactions. In a parallel development, it can be expected that quantum degenerate samples of heteronuclear polar molecules will soon be available through the use of Feshbach resonances [4,5], photoassociation [6,7], or a combination of the two. When in their vibrational ground state, these molecules interact primarily via the electric dipole potential, and they are expected to provide a fascinating new type of dipole-dominated condensates in the near future.

As a result of the anisotropy and long-range nature of the dipole-dipole interaction, a number of phenomena have been predicted to occur in low-density quantum-degenerate dipolar atomic and molecular systems, both in conventional traps and in optical lattices. An early study of the ground state of polar condensates was presented in Ref. [8], which determined its stability diagram as a function of the number of atoms and *s*-wave scattering length. It identified a stable structured ground state for a specific range of parameters. At about the same time, the effect of trap geometry on the stability of the condensate was considered in Ref. [9] for a system dominated by the dipole interaction. This was followed by the prediction [10] of the existence of a number of quantum phases for dipolar bosons in optical lattices. Recent work [11,12] considers the structural phases of vortex lattices in rotating dipolar Bose gases.

A feature of dipolar condensates, as compared to their scalar cousins, is the appearance of a roton minimum in their Bogoliubov spectrum. This feature was discussed in the context of atomic condensates in Ref. [13], which considered the impact of the roton-maxon feature in the excitation spectrum and the stability of pancake-shaped dipolar condensates. For this particular geometry it was found that the excitation spectrum can touch the zero-energy axis for a nonzero wave vector [14], which points to the instability of homogeneous condensates and the onset of density modulations [15]. A roton minimum was also found [16] for the case of laser-induced dipolar interactions in self-bound BECs with cylindrical symmetry. Quasi-2D dipolar bosons with a density-modulated order parameter were determined to be unstable within the mean-field theory [17], and cigar-shaped quasi-one-dimensional condensates were likewise found [18] to be dynamically unstable for dipoles polarized along the axis of the cylindrical trap. The stability of dipolar condensates in pancake traps was also recently discussed in Ref. [21], which found the appearance of biconcave condensates for certain values of the trap aspect ratio and strength of the dipole interaction. From the Bogoliubov excitation spectrum it was possible to attribute the instability of the condensate under a broad range of conditions to its azimuthal component.

Further building on these studies, the present paper reports the results of a detailed numerical analysis of the stability and structure of the Hartree ground state of dipolar condensates confined in anisotropic harmonic trap. We proceed by introducing the trap frequencies ω_x, ω_y, and ω_z, respectively, in the x, y, and z directions, and the corresponding trap aspect ratios $\lambda_y=\omega_y/\omega_x$ and $\lambda_z=\omega_z/\omega_x$. Thus $\lambda_z=1$ corresponds to a pancake trap, whereas $\lambda_z=0$ corresponds to a cylindrical trap with free motion in z direction. We further assume for concreteness that an external field polarizes the dipoles along the y axis. The stability of the condensate is then determined as a function of the trap aspect ratios and of an effective dipolar interaction strength that is proportional to the number of atoms or molecules in the condensate. Various ground-state structures of the condensate are identified in the stable region of parameter space.

The remainder of this paper is organized as follows: Section II introduces our model and comments on important aspects of our numerical approach. Section III summarizes our results, identifying up to five different types of possible ground states, depending on the tightness of the trap and the particle number. Finally, Sec. IV is a summary and conclusion.

II. FORMAL DEVELOPMENT

The dipole-dipole interaction between two particles separated by a distance r is

*Corresponding author. Electronic address: dutta@physics.arizona.edu

$$V_{\rm dd}(r) = g_{\rm dd}\frac{1-3y^2/r^2}{r^3}, \tag{1}$$

where $g_{\rm dd}$ is the dipole-dipole interaction strength and $\hat{y}$ is the polarization direction. For atoms with a permanent magnetic dipole moment we have $g_{\rm dd}=\mu_0\mu_m^2/4\pi$ while for dipolar molecules $g_{\rm dd}=\mu_e^2/4\pi\epsilon_0$, μ_m and μ_e being the magnetic moment of the atoms and the electric dipole moment of the molecules, respectively.

Within the mean-field approximation, the condensate order parameter $\phi(r)$ satisfies the Gross-Pitaevskii (GP) equation

$$E\phi(r) = \left(H_0 + g|\phi^2(r)| + N\int V_{\rm dd}(r-r')|\phi(r')|^2 d^3r'\right)\phi(r), \tag{2}$$

where

$$H_0 = -\frac{\hbar^2}{2m}\nabla^2 + \frac{1}{2}m\omega_x^2(x^2+\lambda_y^2y^2+\lambda_z^2z^2) \tag{3}$$

is the sum of the kinetic energy and the trapping potential and N denotes the number of particles in the condensate. The second term on the right-hand side of Eq. (2) is the contact interaction, $g=4\pi\hbar^2a/m$ being proportional to the s-wave scattering strength a, and the third term describes the effects of the nonlocal dipole-dipole interaction. For dipole interaction dominated systems, g is small compared to $V_{\rm dd}$. This is the case that we consider here, and in the following we neglect the s-wave scattering term altogether.

For convenience we introduce the dimensionless parameter

$$D = Ng_{\rm dd}m/(\ell_x\hbar^2) \tag{4}$$

that measures the effective strength of the dipole-dipole interaction, where the oscillator length $\ell_x=\sqrt{\hbar/(m\omega_x)}$. The condensate ground state is then determined numerically by solving the Gross-Pitaevskii equation (2) for imaginary times. The term involving the dipole interaction energy is calculated using the convolution theorem,

$$\int V_{\rm dd}(r-r')|\phi(r')|^2d^3r' = \mathcal{F}^{-1}\{\mathcal{F}[V_{\rm dd}(r)]\mathcal{F}[|\phi(r)|^2]\},$$

where $\mathcal{F}$ and $\mathcal{F}^{-1}$ stand for Fourier transform and inverse Fourier transform, respectively. The dipole-dipole interaction is calculated analytically in momentum space as [8],

$$\mathcal{F}[V_{\rm dd}(r)] = \frac{4\pi}{3}\left(3\frac{k_y^2}{k_x^2+k_y^2+k_z^2}-1\right), \tag{5}$$

k_x,k_y,k_z are the momentum components in x,y,z direction.

The initial order parameter was chosen randomly, and the stability diagram was generated for each pair of parameters (λ_y,λ_z) by increasing the effective dipolar strength D until a critical value $D_{\rm cr}$ above which the condensate collapses. Because of the random initial condition this value varies slightly from run to run. The plotted results show the average over 100 realizations of the initial wave function, the error bars indicating the maximum deviation of $D_{\rm cr}$ from its mean $\bar{D}_{\rm cr}$. This approach typically resulted in numerical uncertainties similar to those of Ref. [19].

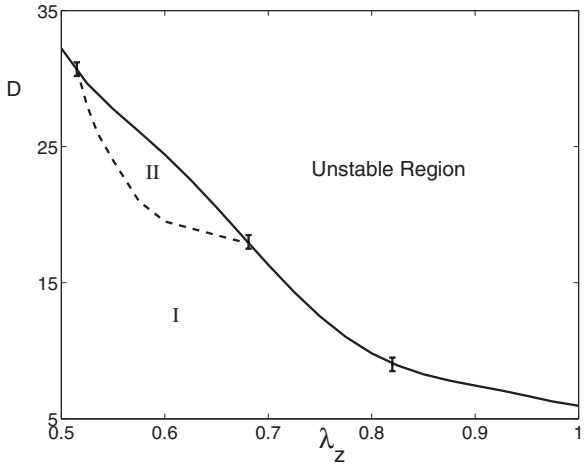

FIG. 1. (λ_z,D) stability diagram of a dipolar condensate in an anisotropic trap for $\lambda_y=5$. The condensate is unstable in the region above the solid line. The dashed line is the boundary between a "structureless Gaussian" and a double-peaked ground-state density profile. The error bars give an indication of the accuracy of the numerical simulations.

III. RESULTS

A good starting point for the discussion of our results is the observation that in the case of a cylindrical trap, $\lambda_z=0$, we found no stable structured condensate ground state. (By structured profiles, we mean profiles that are not simple Gaussians.) In particular, solutions exhibiting density modulations along the z axis were found to be unstable. Moving then to the case of a pancake trap by keeping λ_y fixed but increasing λ_z from 0 to 1, we found for $\lambda_y \gtrsim 4$ the appearance of a small parameter region where the stable ground state is characterized by a structured density profile, the domain of stability of this structured solution increasing with λ_y. A $\{\lambda_z-D\}$ phase space stability diagram typical of this regime is shown in Fig. 1 for $\lambda_y=5$. In this figure, region I is characterized by the existence of a usual condensate with its familiar, structureless Gaussian-like density profile. As λ_z is increased, the condensate becomes unstable for decreasing values of the effective dipole interaction strength D, or alternatively of the particle number N. For $0.525<\lambda_z<0.7$, though, the ground state changes from a Gaussian-shaped to a double-peaked density profile (domain II in the figure), before the system becomes unstable.

Figures 4 and 5show surface plots and corresponding 3D renditions of density profiles typical of the various situations encountered in our study. Figures 4(a) and 5(a) are illustrative of the present case. The appearance of two density peaks away from the center of the trap results from the interplay between the repulsive nature of the dipoles in a plane transverse to its polarization direction, the $(x$-$z)$ plane, and the confining potential.

Increasing the tightness of the trap along the polarization direction y, i.e, increasing λ_y, results in the emergence of

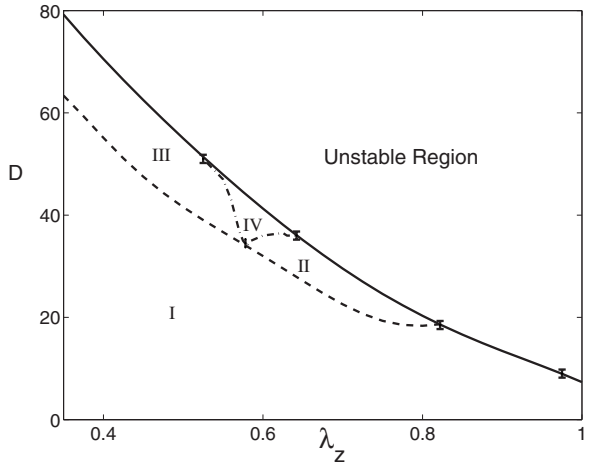

FIG. 2. Stability diagram of a dipolar condensate in an anisotropic trap with $\lambda_y=5.5$, as a function of the dipolar strength D and aspect ratio λ_z. The region above the solid line corresponds to unstable solutions of Eq. (2). The dashed line is the boundary between the structured and the standard ground-state density profiles. The dotted-dashed line marks the boundary between the domains with quadruple-peaked and double-peaked ground-state density profiles.

additional types of structured ground states. One such case is illustrated in Fig. 2, which is for $\lambda_z=5.5$. For small values of λ_z, i.e., a weak trapping potential along the z direction, we observe the appearance of a domain (region III in the figure) characterized by a double-peaked ground state with the maximum density along the z direction and a Gaussian-like density in the x direction. This type of double-peaked structure along the weak trapping axis was first predicted in Ref. [20]. Typical density profiles in this region resemble those in

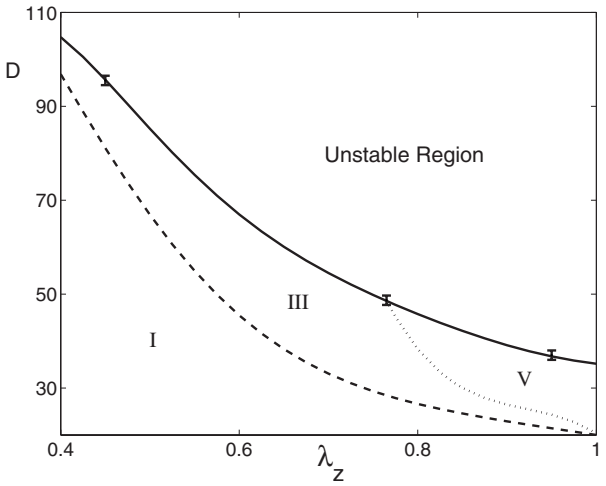

FIG. 3. Stability diagram of a dipolar condensate in an anisotropic trap with $\lambda_y=7$, as a function of the dipolar strength D and the aspect ratio λ_z. The region above the solid line is characterized by unstable ground-state solutions of the mean-field equation (2). The dashed line marks the boundary between a structured and a Gaussian-like ground-state density profile. The dotted line is the boundary between the region with ringlike and two-peaked condensate in the (x-z) plane.

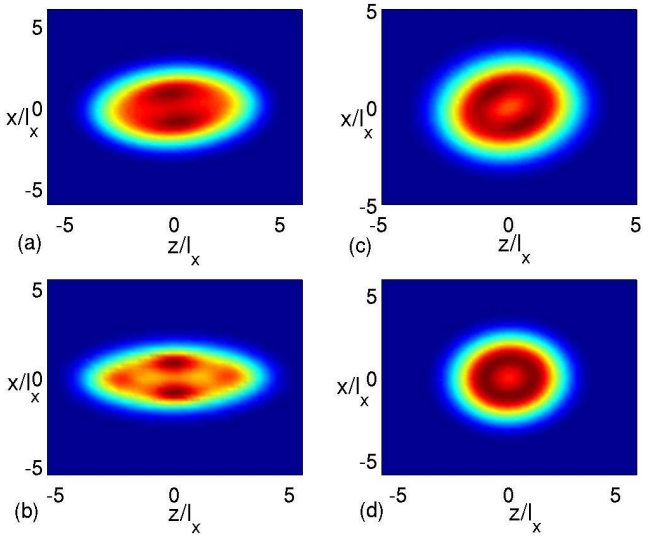

FIG. 4. (Color online) Two-dimensional surface plots of the structured ground-state density profiles typical of various stable domains: (a) Double-peaked density profile in the (x-z) plane for region II, for the parameters $\lambda_y=5$, $\lambda_z=0.6$, and $D=23$. The points of maximum density are away from the trap center and along the x direction. In region (III) the shape of the condensate is similar, but with maximum density along the z direction. (b) Typical quadruple-peaked density profile characteristic of region IV. Here $\lambda_y=5.5$, $\lambda_z=0.575$, and $D=42$. (c) Stable ground-state solution in region V with $\lambda_z<1$. The density is higher and modulated on a radius away from the trap center in the x-z plane. In this example $\lambda_y=7$, $\lambda_z=0.85$, and $D=40$. (d) Density profile typical of the domain V. The condensate is biconcave with maximum density along a constant radius from the trap center. In this example, $\lambda_y=7$ and $D=32$.

Figs. 4(a) and 5(b), but with a rotation by 90 degrees in the (x,z) plane. The regions II and III are separated by a small additional domain IV characterized by a ground-state distribution with a quadruple-peaked structure as illustrated in Figs. 4(b) and 5(b), as might be expected. In general, these characteristics of the ground-state density profile persist until $\lambda_y \approx 6.5$.

Figure 3 shows a stability diagram typical of higher values of the aspect ratio λ_y, in this case $\lambda_y=7$, for $0.4<\lambda_z<1$. As D is increased, the ground-state density of the condensate first undergoes a transition from a Gaussian-like to a double-peaked profile of the type illustrated in Figs. 4(b) and 5(b) (region III). As D is further increased, this domain is followed for λ_z close enough to unity by a second transition to a domain (region V) with the appearance of a density minimum near trap center. Initially, this minimum is surrounded by a region with a radial density modulation, see Fig. 4(c), but for larger values of λ_z this modulation is reduced, see Figs. 4(d) and 5(d). In that region, the density profile resembles the solution previously reported in Ref. [21] for a similar parameter range.

In the case of atoms we have a typical magnetic moment of $6\mu_B$, and we find that the range of critical dipole strengths D corresponding to structured ground states can be achieved for 10^4–10^5 atoms for trapping frequencies $\omega_x \approx 1$ kHz. For molecules with a typical electric dipole moment of 1 Debye the corresponding number is 10^3–10^4 molecules. While

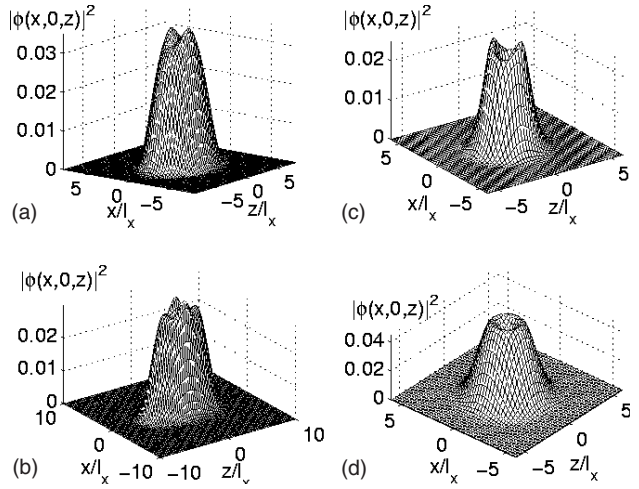

FIG. 5. Three-dimensional ground-state density profile for the same parameters an in Fig. 4.

these are relatively high particle numbers, especially for the atomic case, they do not seem out of reach of experimental realization.

IV. CONCLUSION

In conclusion, we have performed a detailed numerical study of the ground-state structure and stability of ultracold dipolar bosons in an anisotropic trap for dipoles polarized along the y direction. The trap aspect ratios along y and z direction, λ_y and λ_z, were used as control parameters, and the mean-field stability diagram was established as a function of these parameters and a dimensionless interaction strength D. For small λ_y the system was found to exhibit a standard density profile, but for larger values, and depending on λ_z, various structured ground states were found to appear before reaching the unstable regime where the condensate collapses. These include a four-peak structured solution in the x-z plane, a ringlike ground state with a modulated radial density profile. For $\lambda_y \sim 7$ and $\lambda_z = 1$, we found a biconcave condensate profile, as already reported in [21].

For strong confining potentials along the dipole polarization direction, i.e., for large λ_y, increasing λ_z can be viewed as resulting in a change from a quasi-one-dimensional to a quasi-two-dimensional geometry. As such we can think of the various ground-state structures as a result of dimensional crossover in a trapping geometry. To gain a deeper understanding of these structures as we approach the instability region, future work should study the Bogoliubov spectrum of the trapped system.

ACKNOWLEDGMENTS

The authors thank Dr. D. O'Dell, Dr. D. Meiser, and Dr. R. Kanamoto for numerous useful discussions and comments. This work is supported in part by the US Office of Naval Research, the National Science Foundation, the US Army Research Office, the Joint Services Optics Program, and the National Aeronautics and Space Administration.

[1] M. J. Anderson *et al.*, Science **269**, 198 (1995).
[2] K. B. Davis, M. O. Mewes, M. R. Andrews, N. J. van Druten, D. S. Durfee, D. M. Kurn, and W. Ketterle, Phys. Rev. Lett. **75**, 3969 (1995).
[3] A. Griesmaier, J. Werner, S. Hensler, J. Stuhler, and T. Pfau, Phys. Rev. Lett. **94**, 160401 (2005).
[4] C. A. Stan, M. W. Zwierlein, C. H. Schunek, S. M. F. Raupach, and W. Ketterle, Phys. Rev. Lett. **93**, 143001 (2004).
[5] S. Inouye, J. Goldwin, M. L. Oslen, C. Ticknor, J. L. Bohn, and D. S. Jin, Phys. Rev. Lett. **93**, 183201 (2004).
[6] A. J. Kerman, J. M. Sage, S. Sainis, T. Bergeman, and D. DeMille, Phys. Rev. Lett. **92**, 033004 (2004).
[7] J. M. Sage, S. Sainis, T. Bergeman, and David DeMille, Phys. Rev. Lett. **94**, 203001 (2005).
[8] K. Góral, K. Rzażewski, and T. Pfau, Phys. Rev. A **61**, 051601(R) (2000).
[9] L. Santos, G. V. Shlyapnikov, P. Zoller, and M. Lewenstein, Phys. Rev. Lett. **85**, 1791 (2000).
[10] K. Góral, L. Santos, and M. Lewenstein, Phys. Rev. Lett. **88**, 170406 (2002).
[11] N. R. Cooper, E. H. Rezayi, and S. H. Simon, Phys. Rev. Lett. **95**, 200402 (2005).
[12] J. Zhang and H. Zhai, Phys. Rev. Lett. **95**, 200403 (2005).
[13] L. Santos, G. V. Shlyapnikov, and M. Lewenstein, Phys. Rev. Lett. **90**, 250403 (2003).
[14] U. R. Fischer, Phys. Rev. A **73**, 031602(R) (2006).
[15] Y. Pomeau and S. Rica, Phys. Rev. Lett. **72**, 2426 (1994).
[16] D. H. J. O'Dell, S. Giovanazzi, and G. Kurizki, Phys. Rev. Lett. **90**, 110402 (2003).
[17] S. Komineas and N. R. Cooper, Phys. Rev. A **75**, 023623 (2007).
[18] S. Giovanazzi and D. H. J. O'Dell, Eur. Phys. J. D **31**, 439 (2004).
[19] S. Ronen, D. C. E. Bortolotti, and J. L. Bohn, Phys. Rev. A **74**, 013623 (2006).
[20] T. F. Jiang and W. C. Su, Phys. Rev. A **74**, 063602 (2006).
[21] S. Ronen, D. C. E. Bortolotti, and J. L. Bohn, Phys. Rev. Lett. **98**, 030406 (2007).